

MtCRE1-dependent cytokinin signaling integrates bacterial and plant cues to coordinate symbiotic nodule organogenesis in *Medicago truncatula*

Julie Plet¹, Anton Wasson², Federico Ariel³, Christine Le Signor⁴, David Baker⁵, Ulrike Mathesius², Martin Crespi¹ and Florian Frugier^{1,*}

¹Institut des Sciences du Végétal (ISV), Centre National de la Recherche Scientifique, 91198 Gif sur Yvette Cedex, France,

²Australian Research Council Centre of Excellence for Integrative Legume Research, Division of Plant Science, Research School of Biology, Australian National University, Canberra, ACT 0200, Australia,

³Instituto de Agrobiotecnología del Litoral, Consejo Nacional de Investigaciones Científicas y Técnicas – Universidad Nacional del Litoral (CONICET-UNL), Ciudad Universitaria, 3000 Santa Fe, Argentina,

⁴Unité Mixte de Recherche en Génétique et Ecophysiologie des Légumineuses à Graines, Institut National de la Recherche Agronomique, Dijon, France, and

⁵John Innes Genome Laboratory, Norwich NR4 7UH, UK

Received 1 June 2010; revised 17 November 2010; accepted 29 November 2010; published online 18 January 2011.

*For correspondence (fax +33 169 823654; e-mail frugier@isv.cnrs-gif.fr).

SUMMARY

Phytohormonal interactions are essential to regulate plant organogenesis. In response to the presence of signals from symbiotic bacteria, the Nod factors, legume roots generate a new organ: the nitrogen-fixing nodule. Analysis of mutants in the *Medicago truncatula* CRE1 cytokinin receptor and of the MtRR4 cytokinin primary response gene expression pattern revealed that cytokinin acts in initial cortical cell divisions and later in the transition between meristematic and differentiation zones of the mature nodule. MtCRE1 signaling is required for activation of the downstream nodulation-related transcription factors MtERN1, MtNSP2 and MtNIN, as well as to regulate expression and accumulation of PIN auxin efflux carriers. Whereas the MtCRE1 pathway is required to allow the inhibition of polar auxin transport in response to rhizobia, nodulation is still negatively regulated by the MtEIN2/SICKLE-dependent ethylene pathway in *cre1* mutants. Hence, MtCRE1 signaling acts as a regulatory knob, integrating positive plant and bacterial cues to control legume nodule organogenesis.

Keywords: nitrogen fixing nodulation, hormonal interactions, ethylene, EIN2/*sickle*, auxin, PIN efflux carrier.

INTRODUCTION

Legume plants have the ability to develop nitrogen-fixing nodules under starvation conditions and in the presence of a specific bacterial microsymbiont: *Sinorhizobium meliloti* in the case of the model legume *Medicago truncatula*. This symbiotic interaction depends on recognition by host-plants of bacterial Nod factors, which elicits root hair deformations allowing penetration of the bacteria into the epidermis (Oldroyd and Downie, 2008). Simultaneously, nodule organogenesis proceeds from the reactivation of differentiated root inner cortical and pericycle cells in front of protoxylem poles, which divide and lead to the formation of a primordium (Crespi and Frugier, 2008). Rhizobia then progress into infection threads towards the growing primordium, which will subsequently differentiate into a mature

organ. The *M. truncatula* nodule has an indeterminate growth, generating a differentiation gradient initiated from a persistent apical meristem (zone I), and consisting of a region (zone II) where rhizobial infection occurs and cell differentiation is marked by the accumulation of amyloplasts, a functional zone where bacteria are differentiated into bacteroids fixing atmospheric nitrogen (zone III), and a senescence zone (zone IV; Vasse *et al.*, 1990). Many plant mutants unable to nodulate were used to decipher the Nod factor signaling pathways (reviewed in Oldroyd and Downie, 2008), leading to the identification of several downstream transcription factors (TFs): the *nodulation signaling pathway1* (*nsp1*) and *nsp2* mutants affecting GRAS TFs (Kalo *et al.*, 2005; Smit *et al.*, 2005; Heckmann *et al.*, 2006;

Murakami *et al.*, 2006); the *bit1* (*branched infection threads 1*) mutant affecting the AP2/ERF TF MtERN1 (Middleton *et al.*, 2007); and the *nin* (*nodule inception*) putative TF (Schäuser *et al.*, 1998; Marsh *et al.*, 2007).

Appropriate spatio-temporal integration of various cues including phytohormones is essential to determine developmental outputs, as highlighted in the Arabidopsis root model (Benkova and Hejatkó, 2009). For example, cytokinin effects on root elongation and lateral root formation involves regulation of ethylene biosynthesis and the downstream EIN2 signaling pathway (Alonso *et al.*, 1999; Cary *et al.*, 1995; Negi *et al.*, 2008; Ruzicka *et al.*, 2009). In addition, modifications of cytokinin levels or signaling led to changes in PIN expression and protein accumulation in root meristems and lateral root founder cells, likely impacting auxin distribution (Dello Iorio *et al.*, 2008; Laplaze *et al.*, 2007; Negi *et al.*, 2008; Ruzicka *et al.*, 2009). Several phytohormones have been also implicated in the regulation of nodule development. The *M. truncatula sickle* (*skl*) mutant is insensitive to ethylene and presents a hyperinfection phenotype leading to supernodulation (*nod*⁺⁺; Penmetza and Cook, 1997; Penmetza *et al.*, 2003). The *SKL* gene encodes an ortholog of the Arabidopsis Ethylene INsensitive 2 (EIN2) signaling protein (Penmetza *et al.*, 2008). In addition, an inhibition of polar auxin transport (PAT) followed by auxin accumulation in dividing pericycle and cortex cells is a prerequisite for indeterminate nodule initiation (Mathesius *et al.*, 1998; Wasson *et al.*, 2006). This inhibition may involve PIN proteins, as silencing of several of these auxin efflux carriers reduces nodulation (Huo *et al.*, 2006).

Cytokinins play a major role in the control of nodulation (Frugier *et al.*, 2008). Systematic RNAi targeting of the *M. truncatula* cytokinin receptors revealed that the MtCRE1 (Cytokinin Response 1) histidine kinase controls nodule formation (Gonzalez-Rizzo *et al.*, 2006). Similarly, the *Lotus japonicus hit1* (*hyperinfected 1*) mutant carrying a loss of function mutation in the *LHK1* gene (orthologous to MtCRE1) showed strongly reduced nodulation (Murray *et al.*, 2007). The *L. japonicus* phenotype was associated with increased proliferation of infection threads which remained however limited in *M. truncatula* CRE1 RNAi roots. In addition, the *Lotus snf2* gain-of-function mutation affecting the same LHK1 receptor led to cytokinin hypersensitivity and spontaneous nodule formation in the absence of rhizobia (Tirichine *et al.*, 2007). This result indicates that cytokinin signaling is necessary and sufficient to activate cortical cell divisions leading to nodule organogenesis. Genetic interactions showed that the LHK1 pathway acts downstream of Nod factor perception and upstream of the activation of early nodulation-related TFs (Tirichine *et al.*, 2007). Cytokinin signaling relies on a histidine–aspartate multistep phosphorelay ultimately activating type-A response regulators (RRs), which are rapidly transcriptionally induced by cytokinins (Werner and Schmulling, 2009). In *M. truncatula*, the *RR4*

type-A RR is indeed transcriptionally induced by cytokinins and also upregulated upon rhizobial infection depending on the upstream Nod factor signaling (Gonzalez-Rizzo *et al.*, 2006). Conversely, cytokinin regulation of the *NIN* early nodulation marker depends on MtCRE1/LHK1 (Gonzalez-Rizzo *et al.*, 2006; Murray *et al.*, 2007).

Characterization of TILLING mutants affecting the CRE1 cytokinin receptor in *M. truncatula* allowed us to analyze the integration of cytokinins with rhizobial and plant cues in nodule organogenesis. Despite an early inhibition of cortical cell divisions during nodule initiation, *cre1* mutants developed few nodules showing perturbed differentiation and frequently multiple lobes. Accordingly, activation of cytokinin responses occurred both in nodule primordia and in the apical region of mature indeterminate nodules. Analysis of interactions between cytokinins and other cues regulating nodulation revealed that ethylene acts independently of the MtCRE1 cytokinin signaling, whereas this latter pathway acts upstream of auxin, regulating PIN protein expression, accumulation and PAT inhibition in response to rhizobia. Hence, MtCRE1-dependent cytokinin signaling integrates signaling from exogenous Nod factors as well as endogenous cues, such as auxin, to regulate indeterminate nodule organogenesis.

RESULTS

Nodulation phenotypes of a *cre1* mutant allelic series

The kinase domain of the MtCRE1 cytokinin receptor was selected for TILLING (Le Signor *et al.*, 2009). Three single nucleotide mutations introducing either a stop codon in the middle of the kinase domain (*cre1-1*) or single amino acid changes (*cre1-2* and *cre1-3*) were characterized (Figure 1a,b). The *cre1-2* and the *cre1-3* mutations affected, respectively, a conserved residue in the G2 motif and a non-conserved region of the kinase domain. Analysis of root growth sensitivity to cytokinins revealed that both *cre1-1* and *cre1-2* were insensitive to BAP (benzylaminopurine) at 10⁻⁷ M in contrast to the *cre1-3* allele and wild-type controls (Jemalong A17 and a wild-type sibling line of the *cre1-1* allele; Figure 1c,d). We then determined the ability of *cre1* mutants to form symbiotic nodules in response to *S. meliloti* inoculation (Figure 2). In contrast to the *cre1-3* allele, populations segregating *cre1-1* or *cre1-2* showed a strongly impaired nodulation in homozygous mutants (Figure 2a). Use of an *S. meliloti* strain carrying a *Pro*_{HemA}:*LACZ* fusion revealed that infections generally aborted in the epidermis or in the outer cortex, and did not lead to cortical cell division (Figure 2b). In some cases, infection was associated with cortical cell divisions and primordium formation, but infection threads showed many sac-like structures and ramifications despite their capacity to colonize the nodule primordia (Figure 2c). Both *cre1-1* and *cre1-2* alleles can develop a few nodules (Figure 2a), even though their globular shape, when

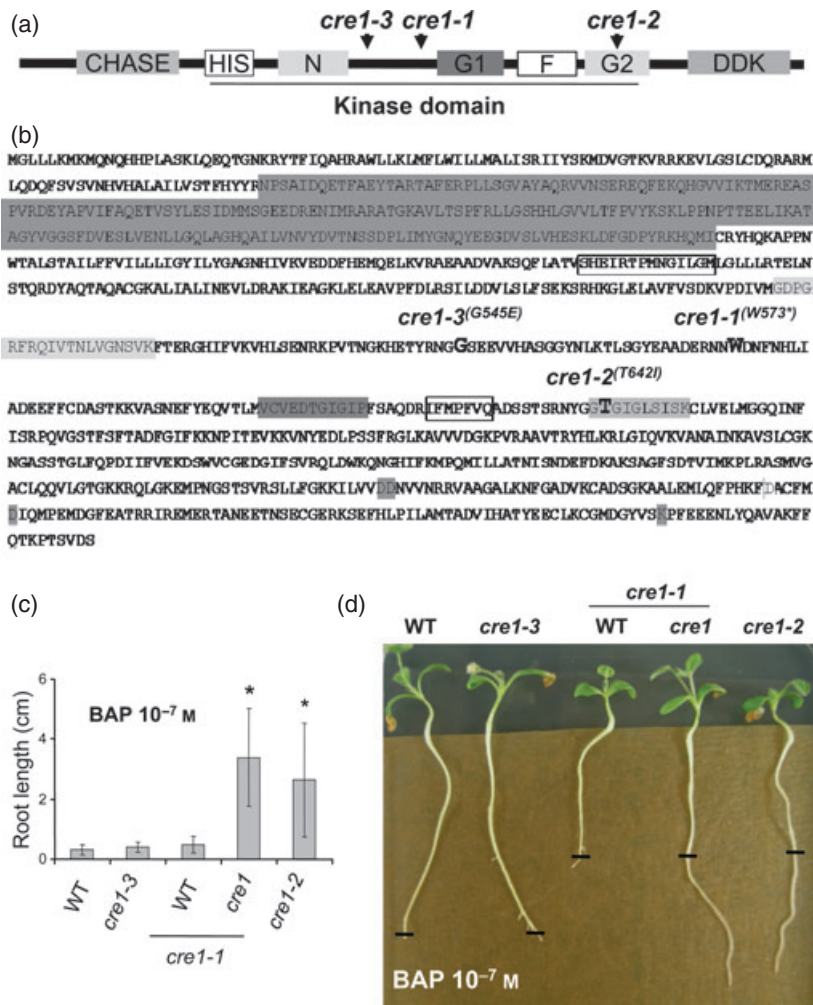


Figure 1. Identification by TILLING of various alleles affecting the kinase domain of the MtCRE1 cytokinin receptor.

(a) Schematic representation of MtCRE1 histidine kinase receptor, highlighting the Cyclase/Histidine kinase Associated Sensory Extracellular (CHASE) domain, different motives of the histidine kinase domain (HIS, N, G1, G2, F; Hwang *et al.*, 2002), and the phosphate acceptor domain (DDK). Arrows indicate location of the three mutant alleles characterized.

(b) Amino acid sequence of the MtCRE1 protein. Boxes and highlights indicate conserved domains/motives following the same code as in (a). Location of mutant alleles is shown with bold residues. *cre1-1* introduces a stop (*) codon, *cre1-2* affects the conserved G2 motif, and *cre1-3* affects a non-conserved residue in the histidine kinase domain.

(c) *cre1-1*, *cre1-2* and *cre1-3* alleles, as well as wild-type (WT) Jemalong seedlings and a WT sibling of the *cre1-1* allele were grown on 'i' medium. Root length was measured 6 days after transfer on BAP 10^{-7} M. Error bars represent confidence interval ($\alpha = 0.05$; $n > 30$) of one representative biological replicate out of three, and a Kruskal–Wallis test was used to assess significant differences ($\alpha < 0.05$).

(d) Representative example of root growth 6 days after transfer on BAP 10^{-7} M for the different *cre1* alleles. Black lines indicate the position of root tips prior to transfer.

compared with the elongated wild-type nodules, confirmed a delayed development (Figure 2d). Histological analysis of wild-type and *cre1* nodules revealed structural differences even when nodules of equivalent sizes were compared (i.e. 20 d.p.i. *cre1* nodules versus 7 d.p.i. wild-type globular nodules; Figure 2e,f). Amyloplast accumulation and autofluorescence associated with rhizobia-infected cells indicated an incomplete differentiation of *cre1* nodules. Later on (2–3 months after inoculation), nodules frequently bare multiple lobes in contrast to the wild-type which were mainly unilobed (Figure S1), suggesting that several meristems were initiated in the mutant nodules.

These results indicate that cytokinins, apart from their crucial role in early steps of nodule organogenesis, may regulate the transition between meristematic and cell differentiation/elongation zones in indeterminate nodules.

Cytokinin responses are activated in dividing cortical cells and in the apical region of mature nodules

To determine the spatio-temporal regulation of cytokinin signaling during nodulation, the A-type Response Regulator

primary cytokinin response gene *MtRR4* was used to generate a transcriptional fusion with the GUS reporter (Figure 3a–f). Histological analysis of *S. meliloti*-inoculated roots showed that the *Pro_{MtRR4}:GUS* fusion was expressed in inner cortex and pericycle (Figure 3a–c), and then in dividing cortical cells and nodule primordia (Figure 3d,e). *Pro_{MtRR4}:GUS* expression was associated in mature nodules with vascular bundles and the apical region (Figure 3f). Use of amyloplasts lugol staining and infected cells autofluorescence as markers revealed that *MtRR4* was expressed both in the meristematic zone I and infection zone II (Figure S2), in agreement with the expression pattern previously identified using *in situ* hybridization (Vernie *et al.*, 2008). To further sustain a role of cytokinins in late nodulation, we analyzed expression patterns of other signaling components (Figure 3g–i). *In situ* hybridization revealed an overlapping expression domain of the MtCRE1 receptor, B-type RRs and A-type RRs in the apical region of differentiated nodules. Hence, late nodulation *cre1* phenotypes correlate with the cytokinin signaling expression domain, suggesting a role of this phytohormone in the regulation of

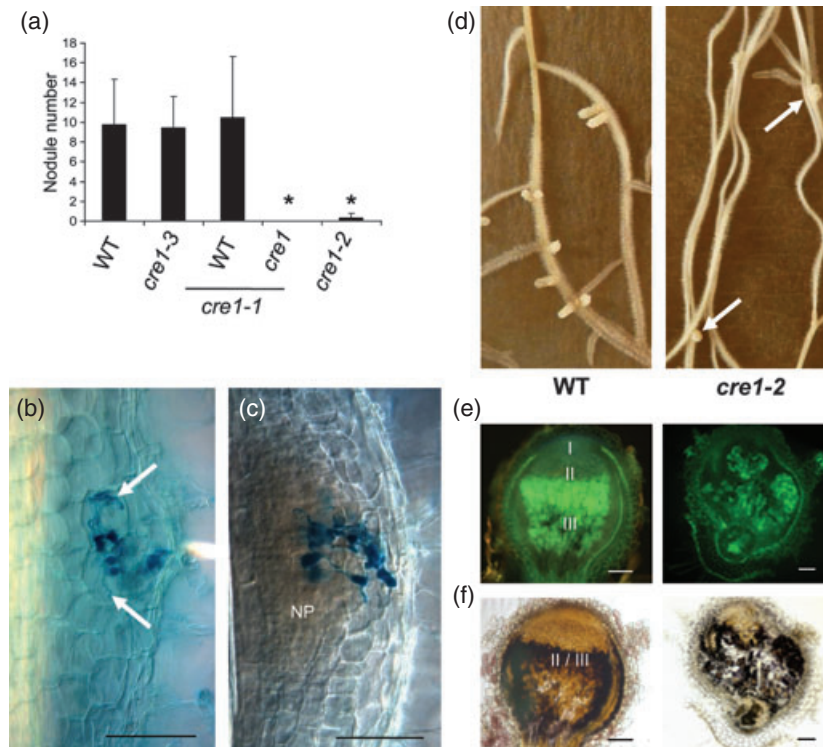


Figure 2. *cre1-1* and *cre1-2* alleles are defective at early and late nodulation stages.

cre1-1, *cre1-2* and *cre1-3* alleles, as well as wild-type (WT) Jemalong seedlings and a WT sibling of the *cre1-1* allele were grown on 'i' medium without nitrogen. (a) Quantification of nodule numbers 15 days post inoculation (d.p.i.) with *S. meliloti* 1021 *in vitro*. Error bars represent confidence interval ($\alpha = 0.05$; $n > 30$) of one representative biological replicate out of three, and a Kruskal–Wallis test was used to assess significant differences ($\alpha < 0.05$). (b, c) Nomarsky bright field image of *cre1-1* roots expressing a *ProHemA::LACZ* reporter and infected with *S. meliloti* (5 d.p.i.). Arrows indicate end of infection threads. NP: nodule primordium. Bar = 100 μm . (d) Representative example of WT (left panel) and *cre1-2* (right panel) *in vitro* grown roots 20 d.p.i. with *S. meliloti* 1021. Arrows point to the few nodules formed on *cre1* roots. (e) Autofluorescence of 7 d.p.i. WT (left panel) and 15 d.p.i. *cre1-2* (right panel) nodule sections, using 450–490 nm excitation/500–550 nm emission filters. Intense green fluorescence mainly reveals cells containing *S. meliloti*. Nodule differentiation is indicated according to Vasse *et al.* (1990): I, meristem; II, infection/differentiation zone; III, nitrogen fixing zone. Bar = 100 μm . (f) Bright field image of 7 d.p.i. WT (left panel) and 15 d.p.i. *cre1-2* (right panel) nodule sections (80 μm) after a lugol staining (same sections as in (e)). Lugol staining reveals amyloplasts in the interzone II/III. Bar = 100 μm .

cell proliferation and/or differentiation in indeterminate nodules.

The MtCRE1-dependent cytokinin pathway is required to regulate Nod factor signaling genes

To analyze the interplay between Nod factors and cytokinins, we determined the cytokinin regulation of TFs acting downstream of this bacterial signal using real time RT-PCR (Figure 4). Similarly to *MtRR4*, a positive control for short-term cytokinin response, the early nodulation-related TFs *MtNIN*, *MtERN1*, and *MtNSP2* were rapidly upregulated in roots exposed to cytokinins, even though various patterns could be identified (Figure 4a). *MtNSP2* showed a transient induction after 1 h of BAP 10^{-7} M treatment but was down-regulated after 3 h, whereas a sustained induction was observed for *MtRR4*, *MtNIN* and *MtERN1*. In contrast to the other transcripts analyzed, *MtNSP1* showed a much weaker regulation by cytokinins. Using a cycloheximide (CHX) pre-treatment, we determined whether these transcriptional

regulations were directly linked to cytokinin signaling (Figure 4b). Besides the *MtRR4* primary cytokinin response gene, none of the nodulation-related TFs tested showed a cytokinin response in presence of CHX indicating that *de novo* synthesis of other regulators was required. As the MtCRE1 cytokinin receptor is essential for nodule organogenesis, we analyzed transcriptional regulations in the *cre1-1* mutant background (Figure 4c). After a short-term cytokinin treatment (BAP at 10^{-7} M for 1 h), regulations of *MtRR4*, *MtERN1*, *MtNSPs* and *MtNIN* were lost in the mutant. Hence, transcriptional regulation of several nodulation-related TFs in response to cytokinins is mainly or even exclusively dependent on the MtCRE1 cytokinin receptor.

Interaction between MtEIN2/SKL-dependent ethylene and MtCRE1-dependent cytokinin pathways during nodulation

In *M. truncatula*, ethylene is a negative regulator of nodule formation (Penmetsa and Cook, 1997). Application of the broadly used ethylene biosynthesis inhibitor AVG

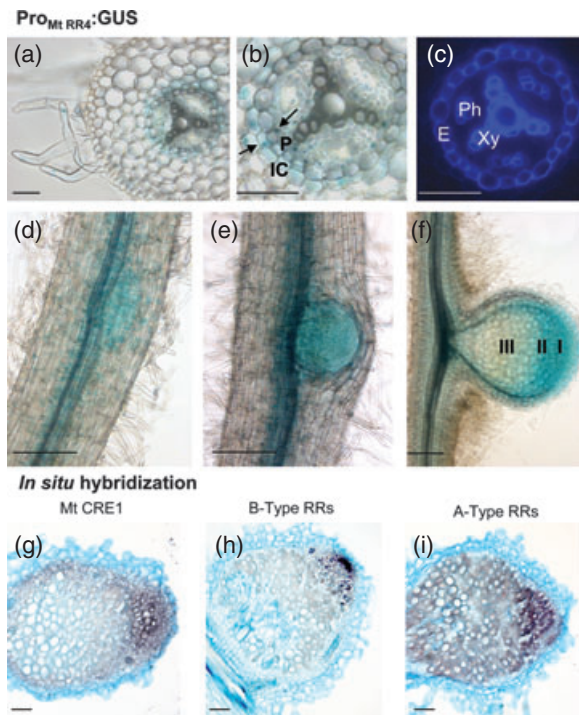


Figure 3. Cytokinin response is activated during nodulation in dividing cortical cells and in the apical region of mature nodules.

(a–f) Localization of *MtRR4* expression using histochemical staining in transversal (a–c) or longitudinal (d–f) sections of roots expressing a *PRO_{MtRR4}:GUS* transcriptional fusion 3 days post inoculation (d.p.i.) with *S. meliloti* 1021. (a, b) Bright field images (b) is a magnification of the root stele region shown in (a). Arrows indicate *PRO_{MtRR4}:GUS* expression in pericycle (P) and inner cortex (IC). (c) Autofluorescence of the section shown in (b), using 340–380 nm excitation/450–490 nm emission filters, highlighting endodermis (e) and vascular bundles (Xy: Xylem and Ph: Phloem). (d–f) Bright field images of a 3 d.p.i. root (d), a 5 d.p.i. nodule primordium (e), and a 7 d.p.i. nodule (f). Nodule zones are shown as described in Vasse *et al.* (1990): I: meristem, II: infection/differentiation zone, III: nitrogen-fixing zone. Bars = 50 μ m in (a–c) and 150 μ m in (d–f).

(g–i) Localization of cytokinin signaling genes expression using *in situ* hybridization on 10 d.p.i. nodules. Antisense probes against the genes indicated were used, and signal corresponds to purple precipitate marking the activity of the alkaline phosphatase detection system. (g) *MtCRE1*; (h) B-Type Response Regulators; and (i) A-Type Response Regulators. Bars = 50 μ m.

(aminoethoxy vinyl glycine) simultaneously to rhizobial infection increased nodulation (Figure 5a). Similarly, *cre1-1* and *cre1-2* mutants showed increased nodulation in the presence of AVG, even though nodule numbers remained strongly reduced compared with the wild-type (Figure 5a). These results suggest that *cre1* mutants are still sensitive to the inhibitory effect of ethylene at early stages of nodule formation.

To analyze more specifically the interactions between cytokinin and ethylene, the *cre1* mutant was crossed to the *sickle* supernodulating mutant affected in the EIN2 ethylene signaling component (Penmetsa *et al.*, 2008). The double mutant *skl/cre1* had a reduced nodulation ability when

compared with the wild-type, but showed enhanced nodulation when compared to *cre1* (Figures 5b and 6a). This finding suggests that the inhibitory EIN2-dependent ethylene pathway acts in parallel to the CRE1-dependent cytokinin pathway to control nodule number. Histology of the few globular nodules formed on *skl/cre1* roots, analyzed using lugol staining and autofluorescence as markers (Figure 6b–d), showed that nodule zonation in *skl/cre1* is more similar to *skl* than to *cre1*. Indeed, lugol staining clearly identified the meristematic and infection regions (zones I and II) in contrast to *cre1* nodules where the differentiation gradient was perturbed.

Overall, the epistatic interactions between *skl* and *cre1* along nodulation point to different outputs of the cytokinin and ethylene interplay at various developmental stages.

MtCRE1 signaling is required to regulate specific PIN efflux carriers accumulation and *Rhizobium* inhibition of polar auxin transport

As PAT was shown to be crucial for indeterminate nodule formation, we analyzed by real-time RT-PCR expression of six PIN auxin efflux carriers detectable in *M. truncatula* roots and nodules (based on Schnabel and Frugoli, 2004; Table S1). In response to a short-term exogenous cytokinin treatment, no major change in *PIN* expression was observed in whole roots, except for *MtPIN9* (a homolog of *AtPIN5*; Schnabel and Frugoli, 2004) which was strongly downregulated (Figure S3a–c). Steady state levels of *PIN* expression were determined in wild-type and *cre1* roots, revealing a significant accumulation of *MtPIN3* and *MtPIN6* transcripts and reduced *MtPIN9* levels in the mutant background (Figure 7a), mainly observed in root apices (Figure S4). We then developed an antibody (PIN62, see Experimental procedures) able to recognize most of the *Medicago* PIN auxin efflux carriers homologous to Arabidopsis proteins polarly localized in plasma membranes and proposed to be crucial for PAT (i.e. against the *Medicago* orthologs of *AtPIN1* to 4, *AtPIN6* and *AtPIN7*; Table S1; Petrasek and Friml, 2009). As expected, analysis of *PIN* localization pattern in wild-type *Medicago* roots revealed membrane polarly-localized signals (Figure 7b). Interestingly, *PIN* proteins were notably detected in inner cortical cell layers (Figure 7c), and stronger signals were observed in *cre1* root apices (Figures 7d,e; a quantification of *PIN*-polar signals is provided in Figure S5). To further support this result, we analyzed PAT in wild-type and *cre1* roots. Direct acropetal auxin transport measurements revealed that *cre1* roots have an increased PAT rate (Figure 7f). In addition, the PAT inhibition observed in wild-type in response to *S. meliloti* inoculation was not detected in *cre1* (Figure 7g). We then determined whether this deregulation was correlated with changes in *PIN* expression under symbiotic conditions. Whereas a high variability of *PIN* expression patterns was observed a few hours after rhizobia inoculation (data not shown), a significant accumulation of

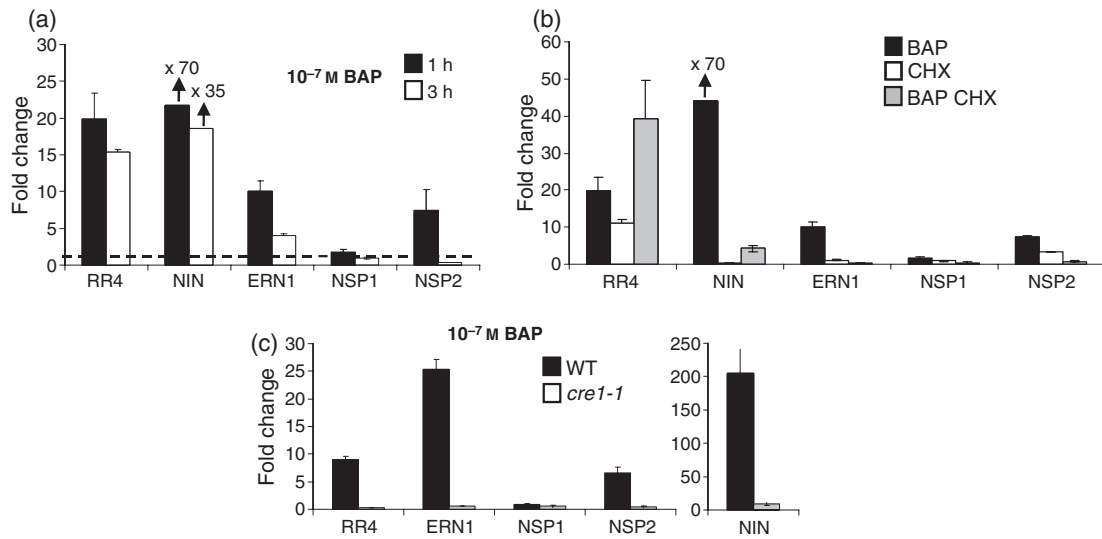


Figure 4. Downstream transcription factors involved in Nod factors signaling pathways are regulated by cytokinins depending on MtCRE1.

(a) Real time RT-PCR analysis of *MtRR4*, *MtNIN*, *MtERN1*, *MtNSP1*, and *MtNSP2* expression in roots treated for 1 or 3 h with BAP 10^{-7} M. (b) Real time RT-PCR analysis of *MtRR4*, *MtNIN*, *MtERN1*, *MtNSP1*, and *MtNSP2* expression in roots treated for 1 h with BAP 10^{-7} M, with or without a 1 h pre-treatment with cycloheximide (CHX) $50 \mu\text{M}$. A 1 h CHX pre-treatment control was also included. (c) Real time RT-PCR analysis of *MtRR4*, *MtNIN*, *MtERN1*, *MtNSP1*, and *MtNSP2* expression in wild-type (WT) and *cre1-1* roots in response to a 1 h BAP 10^{-7} M treatment.

In all cases, expression was normalized with values of the non-treated condition for each gene, to show fold changes (a ratio of 1 is indicated by the dotted line). Three reference genes (defined using Genorm software as non-BAP- and non-CHX-regulated; see Experimental procedures) were used. Error bars represent standard deviation of two technical replicates, and one representative biological replicate is shown out of three.

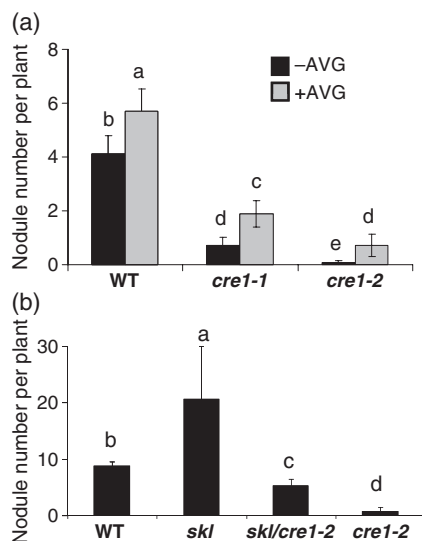


Figure 5. Interactions between cytokinins and ethylene pathways during nodulation.

(a) Quantification of nodule number 7 days post inoculation (d.p.i.) with *S. meliloti* 1021 in wild-type (WT) Jemalong, *cre1-1* and *cre1-2* mutants in presence or absence of the ethylene biosynthesis inhibitor AVG (10^{-6} M). Error bars represent confidence interval ($\alpha = 0.05$; $n > 30$) of one representative biological replicate out of three, and a Kruskal–Wallis test was used to assess significant differences ($\alpha < 0.05$).

(b) Quantification of nodule number 7 d.p.i. with *S. meliloti* 1021 in WT, *cre1-2*, *sickle-1* (*skl*) and *skl/cre1-2* double mutants. Error bars represent confidence interval ($\alpha = 0.05$; $n > 30$) of one representative biological replicate out of three, and a Kruskal–Wallis test was used to assess significant differences ($\alpha < 0.05$).

MtPIN4 and *MtPIN10* transcripts and a decreased level of *MtPIN9* expression were detected in response to a Nod factor treatment (10^{-8} M, 1–6 h) in wild-type roots (Figure 7h). In the *cre1-1* mutant, *MtPIN9* downregulation was significantly retrieved, and similar trends were observed for *MtPIN4* and *MtPIN10*, indicating that a regulation of *PIN* expression by Nod factors still occurred in *cre1*.

Hence, PAT regulation in roots depends on the MtCRE1 cytokinin pathway both under symbiotic and non-symbiotic conditions, as well as changes in the expression and accumulation of specific PIN auxin efflux carriers.

DISCUSSION

Our work showed various roles for cytokinins and their interactions with different cues during nodule organogenesis, from initiation of cortical cell divisions to regulation of nodule growth and differentiation. Two of the *cre1* TILLING alleles identified in this study, one of those generating a nonsense mutation, showed similar cytokinin insensitivity and nodulation phenotypes. In both alleles, no obvious phenotype was detected in shoots, reinforcing that MtCRE1 has a major contribution in below-ground organs development. As previously shown in CRE1 RNAi roots infected by *S. meliloti* (Gonzalez-Rizzo *et al.*, 2006), infection threads were mainly blocked in the *cre1* mutant epidermis, and no extensive invasion of outer root cell layers was observed. In the few cases where primordia formed, infection threads developed many sac-like structures and ramifications, and

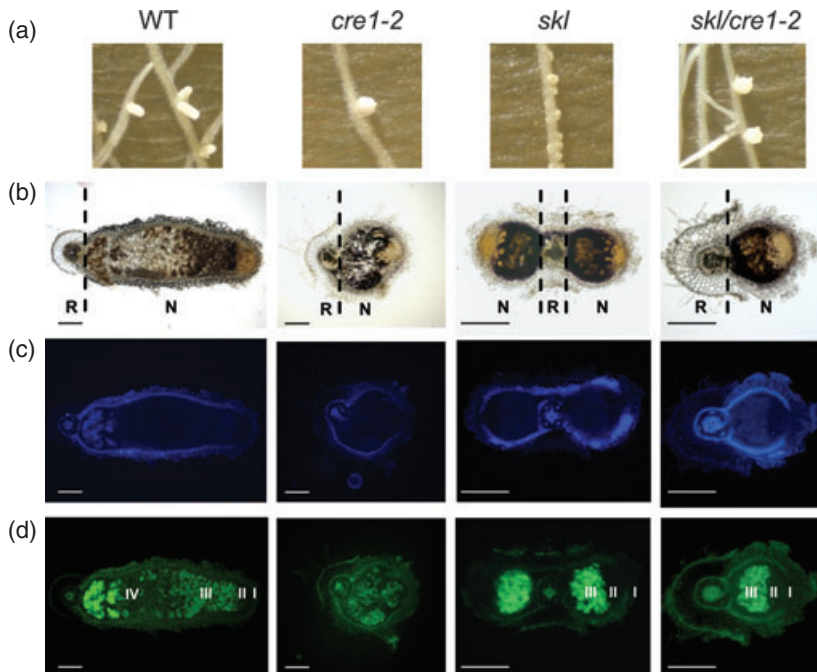


Figure 6. Nodulation phenotypes of the *cre1/sickle* double mutant.

(a) Phenotypes of nodules from wild-type (WT) Jemalong, *cre1-2*, *sickle-1 (skl1)*, and *skl1/cre1-2*, 20 days post-inoculation (d.p.i.) with *S. meliloti* 1021.

(b–d) Sections of 20 d.p.i. nodules from WT, *cre1-2*, *sickle-1 (skl1)*, and *skl1/cre1-2*. (b) Bright field images of root (R) and nodule (N) sections (80 µm) after a lugol staining. Lugol staining reveals amyloplasts as a marker of differentiation. (c) Autofluorescence of nodules using 340–380 nm excitation/450–490 nm emission filters, mainly revealing the presence of autofluorescent flavonoids and endodermis. (d) Autofluorescence of nodules using 450–490 nm excitation/500–550 nm emission filters, mainly highlighting cells infected by *S. meliloti*. Nodule differentiation is indicated according to Vasse *et al.* (1990): I, meristem; II, infection/differentiation zone; III, nitrogen fixing zone; IV, senescence zone. Bars = 150 µm.

infection was delayed. In *L. japonicus*, cytokinin pathways activation in the epidermis was proposed based on the use of the Arabidopsis *ProARR5::GUS* fusion (Lohar *et al.*, 2004). Analysis of soybean root hair transcriptome in response to rhizobia did not reveal however any enrichment for endogenous transcripts related to cytokinin signaling (Libault *et al.*, 2010). Using the endogenous *MtRR4* primary cytokinin response gene, we showed that an activation of cytokinin pathways occurred in inner cortex and pericycle but not in outer cortex or epidermis where most of *cre1* infections were blocked. Accordingly, expression of *MtCRE1* was previously detected in cortical cells but not in the epidermis (Lohar *et al.*, 2006). These results support that in *Medicago*, cytokinins primarily act in dividing inner cortical cells. Interestingly, the functionally related LHK1 pathway in *L. japonicus* was recently unambiguously associated to nodule organogenesis acting in the cortex, based on genetic interactions (Madsen *et al.*, 2010). The contrasting cytokinin responses observed in *Lotus* and *Medicago* epidermis may reflect different functions for this phytohormone depending on host-plants and/or in feedback mechanisms generated by dividing cortical cells to control epidermal infection. Interestingly, hyperinfection is observed in *M. truncatula skl* ethylene-insensitive mutant but not in *cre1*, whereas a hyperinfection phenotype was reported in the *L. japonicus* cytokinin insensitive *hit1* mutant (for *hyper infection threads*; Murray *et al.*, 2007), but not in the recently identified ethylene insensitive *enigma* mutant affecting *LjEIN2* (Gresshoff *et al.*, 2009). In contrast, *enigma* mutants are defective in nodulation and infection thread formation. More generally, the variety of nodule organogenesis (i.e. cell

divisions activated in outer versus inner cortex, or determinate versus indeterminate growth) are likely linked to different requirements for phytohormonal regulations.

In *Lotus* and *Medicago*, mutants affecting CRE1/LHK1 are similarly able to develop a few nodules. *cre1* nodule organogenesis was delayed, leading to differentiation defects and formation of multiple lobes, which correlated with the expression of cytokinin signalling components in the nodule apical region. The increased *cre1* nodule size may be however partly explained by a compensation effect of the low nodule number, as reported in other mutants (Libault *et al.*, 2009; Magori *et al.*, 2009). In Arabidopsis roots, cytokinins promote the exit of cells from meristems to elongate and differentiate (Dello iolo *et al.*, 2007). Our results suggest that cytokinins may act in mature nodules to regulate the balance between cell proliferation and differentiation.

Many early nodulation markers are transcriptionally regulated by cytokinins (Frugier *et al.*, 2008), including *MtNIN* whose regulation depends on the *MtCRE1/LHK1* pathway (Gonzalez-Rizzo *et al.*, 2006; Murray *et al.*, 2007). We now show that other TFs transcriptionally regulated by rhizobia and acting upstream of NIN are regulated by cytokinins through CRE1. In all cases however, *de novo* synthesis of other transcriptional components was required for this activation. Interestingly, *MtNSP2*, one of the most upstream TF acting in early Nod factors signaling both in cortical and epidermal cells (Oldroyd and Downie, 2008) shows a very dynamic regulation by cytokinins. The *MtERN1* TF has been primarily linked to infection thread formation and *ENOD11* expression in root hairs (Andrianakaja *et al.*, 2007; Middleton

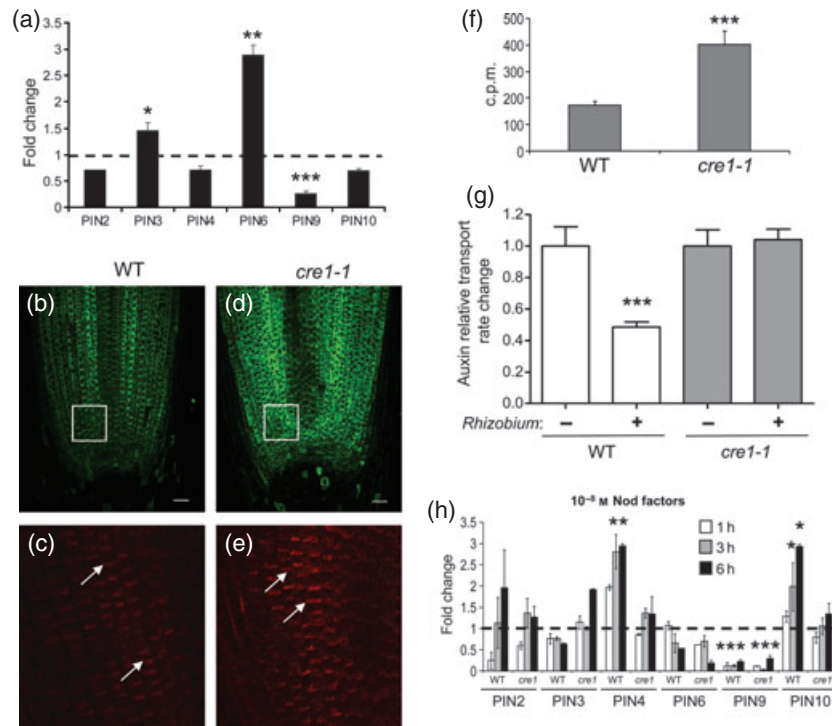


Figure 7. *Rhizobium* inhibition of polar auxin transport depends on the MtCRE1 cytokinin pathway.

(a) Real-time RT-PCR analysis of MtPIN expression in wild-type (WT) and *cre1-1* whole roots. Three reference genes (defined using Genom software as non-regulated between *cre1* and WT; see Experimental procedures) were used. *cre1*/WT ratio are shown (a ratio of 1 is indicated by the dotted line), error bars represent standard deviation of two technical replicates, and one representative biological replicate is shown out of four. A Mann–Whitney test was used to assess significant differences based on values obtained in the biological replicates (*, $\alpha < 0.05$; **, $\alpha < 0.01$; and ***, $\alpha < 0.001$).

(b–e) Representative images of *M. truncatula* PIN proteins immunolocalization in wild-type (WT) Jemalong (b, c) or *cre1-1* (d, e) root apex. A primary antibody (PIN62) designed to recognize all PINs predicted to locate on plasma membranes was used (1:500), followed by an Alexa488 (b, d) or Alexa568 (c, e) secondary antibody (1:1000). For (b, d) and (c, e) respectively, pictures have been taken using the same confocal acquisition settings. In (c) and (e) are shown details of the inner cortex. Arrows point to polar localization of PINs in plasma membranes. Bars = 50 μm .

(f) Quantification (in counts per minute, or c.p.m.) of acropetal polar auxin transport using radiolabelled IAA in WT or *cre1-1* root apex at 8–12 mm distance from the root tip. Error bars represent standard error of the mean ($n > 27$) of one representative biological replicate out of three, and a Student's *t*-test was used to assess significant differences ($P < 0.001$).

(g) Quantification of polar auxin transport using radiolabelled IAA in WT or *cre1-1* root segments just below the point of inoculation with rhizobia 24 h.p.i. Data are normalized against values of each non-inoculated control to highlight effect of *Rhizobium* inoculation. Error bars represent standard error of the mean ($n > 27$) of one representative biological replicate out of three, and a Student's *t*-test was used to assess significant differences ($P < 0.001$) between control and inoculated conditions.

(h) Real-time RT-PCR analysis of MtPIN expression in wild-type or *cre1-1* roots treated for 1, 3 or 6 h with Nod factors 10^{-8} M purified from *S. meliloti*. In all cases, expression was normalized with values of the non-treated condition for each gene, to show fold changes (a ratio of 1 is indicated by the dotted line). Three reference genes (defined using Genom software as non-regulated by Nod factors; see Experimental procedures) were used. Error bars represent standard deviation of two technical replicates, and one representative biological replicate is shown out of two. A Mann–Whitney test was used to assess significant differences based on values obtained in the biological replicates (*, $\alpha < 0.05$; **, $\alpha < 0.01$; and ***, $\alpha < 0.001$).

et al., 2007), but is however also expressed in spontaneous nodules formed in the absence of *Rhizobium* (Gleason *et al.*, 2006). Similarly, NIN is associated with epidermal and cortical responses (Marsh *et al.*, 2007). Based on our results, it is likely that the CRE1-dependent early induction of these nodulation-related TFs by cytokinins takes place in the cortex to activate nodule organogenesis.

Appropriate spatial and temporal regulation of signaling pathways and their interactions is essential to determine developmental outputs. In *Arabidopsis* roots, an interplay between auxin, ethylene and cytokinins occurs, ethylene controlling root elongation and lateral root formation

through complex interactions with auxin biosynthesis and polar transport (Benkova and Hejatko, 2009; Negi *et al.*, 2008). Our results show that, in *cre1*, nodulation is still repressed even if the ethylene pathway is inhibited through mutation of *ein2/skl*. Previously, the expression domain of an ACC oxidase enzyme, catalyzing ethylene biosynthesis, was localized between protoxylem poles, and negatively correlating with nodule initiation sites (Heidstra *et al.*, 1997). The spatial regulation exerted by ethylene on nodule initiation may then restrict the domain where activation of cytokinins should occur, i.e. in cells in front of protoxylem poles. Our results additionally suggest that in mature

indeterminate nodules, the balance between proliferation and differentiation may involve interactions between ethylene and cytokinins.

Auxin was recently shown to activate A-type ARR expression in the basal pole of Arabidopsis embryos corresponding to root stem cells, potentially leading to an inhibition of the cytokinin pathway (Muller and Sheen, 2008). Conversely, exogenously applied cytokinins regulate the spatiotemporal accumulation of PIN auxin efflux carriers in roots, suggesting that endogenous levels of cytokinins perturb auxin fluxes necessary for lateral root initiation (Laplaze *et al.*, 2007) and to determine root meristem size and growth rate (Dello Iorio *et al.*, 2008; Ruzicka *et al.*, 2009). AtPIN1, PIN3 and PIN7 were accumulated in the root apex of the *ahk3* (*authentic histidine kinase 3*) mutant, and their regulation by cytokinins was impaired in various cytokinin receptor mutant combinations. In *Medicago cre1* root apices, a higher accumulation of PIN proteins was detected, notably in the inner cortex that is involved in nodule organogenesis. In addition, analysis of individual *PIN* gene expression revealed increased levels of MtPIN3 and MtPIN6 transcripts in *cre1* roots. These expression patterns correlated with an increased PAT capacity of *cre1* roots, likely leading to an increased accumulation of auxin in apices. The lack of PAT inhibition in response to rhizobia inoculation observed in *cre1* further revealed that MtCRE1-dependent cytokinin signaling acts upstream of auxin-related pathways crucial for root and nodule organogenesis. The different *PIN* genes changing expression after a short-term Nod factor treatment do not however correspond to the ones whose transcripts accumulate in the *cre1* mutant. Moreover, similar regulations were retrieved in the *cre1* mutant, even though not significant for MtPIN4 and MtPIN10, indicating that response to Nod factors may be fainter or delayed in the mutant. In Arabidopsis, post-transcriptional modifications, such as phosphorylation, have been linked to PIN proteins function (Titapiwatanakun and Murphy, 2009), and these levels of regulation may be also involved in the response to rhizobia. In addition, other components of the PAT machinery or of the auxin response may be required for symbiotic nodule organogenesis depending on the CRE1 pathway. Finally, we cannot discard the hypothesis that *cre1* roots may have become resistant to the PAT inhibition induced upon symbiotic bacteria inoculation indirectly, due to their increased auxin flux associated to the accumulation of PINs in the meristematic region.

Overall, our results show that MtCRE1 signaling integrates positive bacterial and plant cues (i.e. Nod factors and auxin) to temporally and spatially regulate nodule initiation. In addition, cytokinins and their interactions likely exert a continuous control on differentiation and growth of indeterminate nodules. Coordinated regulation of the cytokinin response by the host plant and its symbiont is therefore a crucial target to control various stages of nodulation, and

may also be essential to determine the different types of nodule organogenesis and growth.

EXPERIMENTAL PROCEDURES

Biological material

Medicago truncatula Jemalong A17 seeds were sterilized for 20 min in bleach (12% [v/v] sodium hypochlorite). After washing with sterilized water, seeds were sown on 1% agar plates, stored for 2 days at 4°C before incubating overnight at 24°C in the dark. Germinated seedlings were transferred to square plates containing appropriate medium (see below) and grown vertically in chambers at 24°C under long-day conditions (16 h light at 150 µE light intensity/8 h dark).

cre1 mutant alleles *cre1-1*, *cre1-2*, and *cre1-3* were identified in this study by TILLING (Le Signor *et al.*, 2009; primers indicated in Table S2). A wild-type sibling line of the *cre1-1* allele was also used as control. In addition, the *skl-1* mutant (Penmetsa and Cook, 1997; Penmetsa *et al.*, 2008) was used to generate the *skl-1/cre1-2* double mutant. The *cre1-1* allele was backcrossed successively two times with Jemalong A17, and both *cre1-1* and *cre1-2* alleles were systematically used for phenotyping. *cre1* genotyping was done using PCR with the same primers as the one used for TILLING and subsequent sequencing. Alternatively, based on these amplicons, a *Bfa*I restriction was used to genotype *cre1-1* (as the mutation generated such restriction site); a *Kpn*I restriction to genotype *cre1-2* (as the mutation deleted this restriction site); and a *Mnl*I restriction to genotype *cre1-3* (as the mutation deleted this restriction site). *skl* genotyping was done using PCR (primers indicated in Table S2) and subsequent sequencing.

For nodulation experiments, germinated seeds were grown *in vitro* on low-nitrogen liquid medium ('i'; Blondon, 1964). Roots were inoculated with 10 ml of *Sinorhizobium meliloti* suspension (OD₆₀₀ = 0.05) per plate for 1 h. Different bacterial strains were used: a wild-type Sm1021 strain and a derivative strain (GMI6526; Ardourel *et al.*, 1994) carrying the pXLGD4 plasmid containing a *Pro_{HemA}:LACZ* transcriptional fusion. Nod factors were extracted from *S. meliloti* Sm2011 (GMI6390, pMH682) following the protocol described in Roche *et al.* (1991).

Hormonal and Nod factors treatments

Fifteen germinated seedlings were placed on a grid in a Magenta box with 30 ml of low-nitrogen 'i' liquid medium and grown in a shaking incubator (125 g) at 24°C under long-day conditions (16 h light/8 h dark). After 5 days, seedlings were treated with or without BAP (Sigma-Aldrich, <http://www.sigmaaldrich.com/>) at 10⁻⁷ M and maintained under the same growth conditions for various incubation times (0, 1 and 3 h). Similarly, Nod factors purified from *S. meliloti* were used at 10⁻⁸ M for 1, 3 or 6 h. A 1 h CHX (Sigma-Aldrich) 50 µM pre-treatment was also used in some experiments. Roots were collected at the indicated time points and immediately frozen in liquid nitrogen for RNA extraction. In all cases, three independent biological experiments were performed.

To test the sensitivity of the *cre1* mutant roots to cytokinins and the effect of the ethylene biosynthesis inhibitor AVG (Sigma-Aldrich), roots were grown on growth papers (Mega International, <http://www.mega-international.com/index.htm>) placed on 'i' medium. After 3 days, plants were transferred on a fresh 'i' medium supplemented or not with BAP at 10⁻⁷ M or with AVG at 10⁻⁶ M. For cytokinin sensitivity, position of root tips was marked at the time of transfer, and root growth from this point was measured after 6 days using ImageJ software (<http://rsbweb.nih.gov/ij/>). Three independent biological replicates were performed for each experiment.

Gene expression analysis

Total RNA was extracted from frozen roots using the RNeasy plant mini kit (Qiagen, <http://www.qiagen.com/>). First-strand cDNA was synthesized from 1.5 µg of total RNA using the Superscript II first-strand synthesis system (Invitrogen, <http://www.invitrogen.com/>). Primer design was performed using Primer3 software (<http://frodo.wi.mit.edu/cgi-bin/primer3/>). Primer combinations showing a minimum amplification efficiency of 90% were used in real-time RT-PCR experiments (Table S2). Real-time RT-PCR reactions were performed using the LightCycler FastStart DNA Master SYBR Green I kit on a LightCycler apparatus according to manufacturer's instructions (Roche, <http://www.roche.com/>). Cycling conditions were as follows: 95°C for 10 min, 50 cycles at 95°C for 5 sec, 58°C for 5 sec, and 72°C for 15 sec. PCR amplification specificity was verified using a dissociation curve (55–95°C). A negative control without cDNA template was always included for each primer combination. Technical replicates (on two independent syntheses of cDNA derived from the same RNA sample) and three independent biological experiments were performed in all cases. Ratios were done with constitutive controls for gene expression to normalize the data between different biological conditions. MtACTIN11, MtRBP1 and MtH3L were selected using Genorm software (<http://medgen.ugent.be/~jvdesomp/genorm/>; Vandesompele *et al.*, 2002) as reference genes for experiments involving hormonal treatments in wild-type and *cre1* mutant roots (primers shown in Table S2). MtRBP1 was chosen to calculate ratios, and the value of the experimental control condition was set up to 1 as a reference to determine relative expression or induction factors. When weak changes in expression were observed, a Mann–Whitney test (available in the XLstat software; <http://www.xlstat.com/>) was used to assess significant differences based on the different biological replicates performed.

In situ hybridizations were performed as described in Valoczi *et al.* (2006) on 15 d.p.i. nodules using an Intavis InsituPro automat (<http://www.intavis.com/en/>). Sense and antisense RNA probes corresponding to a carbonic anhydrase gene (MtCa1) were included as negative and positive controls, respectively (Coba de la Pena *et al.*, 1997; Boualem *et al.*, 2008). A probe specifically directed against MtCRE1 was designed whereas, due to the extensive homology among B-type or among A-type RRs (Gonzalez-Rizzo *et al.*, 2006), we could not find a discriminatory region for probing each individual gene. A nucleotide identity lower than 70% between A- and B-type RRs in the regions used as probes allowed however to discriminate each family. All probes used are listed in Table S2.

Agrobacterium rhizogenes root transformation

A 3030 bp sequence upstream of the MtRR4 start codon was amplified by PCR using a *Pfx* polymerase (Invitrogen) and primers MtRR4-5' and MtRR4-3' (Table S2). PCR product was subsequently cloned using Gateway technology (Invitrogen) into the pKGWFS7 vector (<http://www.psb.ugent.be/gateway/index.php>) carrying a GFP–GUS fusion downstream of the cloning recombination site. The resulting constructs were introduced into *Agrobacterium rhizogenes* ARqua1 (Quandt *et al.*, 1993) and used for *M. truncatula* root transformation. The transgenic roots were obtained after kanamycin (25 mg/L) selection for 2 weeks as described by Boisson-Dernier *et al.* (2001). Composite plants were then transferred onto growth papers (Mega International) on Fahraeus medium without nitrogen (Truchet *et al.*, 1985) for 4 days. Thereafter, the transgenic roots were inoculated with an *S. meliloti* 1021 strain. Roots or nodules were collected at 3, 5, 7, and 15 d.p.i. for histochemical GUS analysis. Three independent biological experiments were performed ($n > 20$).

Histochemical stainings and microscopic analyses

Histochemical staining for GUS activity was performed as previously described (Pichon *et al.*, 1992; samples were incubated for up to 24 h at 37°C). After staining, nodules were included in 3% agarose and then sliced into 80-µm sections using a VT 1200S vibratome (Leica Microsystems, <http://www.leica-microsystems.com/>). A 5 min staining with lugol (Sigma-Aldrich) was used to detect amyloplasts. When necessary, samples or sections were cleared briefly with sodium hypochlorite, as described in Pichon *et al.* (1992), and observed in bright field using a DMI6000B microscope equipped with a DFC300 camera (Leica Microsystems).

Roots and nodules infected by the Sm1021 strain expressing the *Pro_{Hema}:LACZ* were used for β-galactosidase staining, as described in Ardourel *et al.* (1994). Stained samples were observed in bright field with a Reichert Polyvar microscope equipped with a QImaging Retiga2000 Camera (<http://www.qimaging.com/>).

For histological analysis, autofluorescence of vibratome sections mounted in water was observed using 450–490 nm excitation/500–550 nm emission filters (green fluorescence of nodule infected cells) or 340–380 nm excitation/450–490 nm emission filters (blue fluorescence of endodermis and flavonoids) on a DMI6000B microscope equipped with a DFC300 camera (Leica Microsystems).

Generation of an antibody recognizing MtPINs proteins and immunolocalization

An antibody able to recognize most of the predicted plasma-membrane located *Medicago* PIN proteins, referred to as 'PIN62' antibody, was generated based on immunization of two rabbits using the TPRASNLNAEI peptide coupled to the KLH carrier, following a typical Eurogentec immunization protocol (<http://www.eurogentec.com/>). The sera obtained were purified against the peptide and subsequently tested in ELISA to determine their sensitivity in comparison to pre-immune sera.

One-day-old seedling roots were fixed in 4% PFA using a vacuum desiccator and after inclusion into 3% agarose, root tips were longitudinally sliced into 80-µm sections using a vibratome (Leica VT 1200S, Leica Microsystems). Immunodetection was performed using an Intavis InSituPro automat as described in Friml *et al.* (2003). PIN62 antibody was used at a dilution of 1:500, and anti-rabbit-Alexa488 or anti-rabbit-Alexa568 secondary antibodies (Invitrogen) were used at 1:1000. Pre-immune serum gave no detectable signal. After excitation at 488 nm or 568 nm, emission of the fluorochrome was detected respectively between 500 and 544 nm or 595 and 610 nm on a SP2 Inverted Confocal Microscope (Leica Microsystems). Quantification of the intensity of PIN polar signals was measured using ImageJ on images obtained using the same confocal configuration for wild-type and *cre1-1* root vibratome sections ($n = 4$ sections/genotype from two independent biological replicates; and $n = 30$ cells/section).

Polar auxin transport measurements

Auxin transport experiments were done as described by Wasson *et al.* (2006) with the following modifications. Five-day-old *in vitro* grown seedlings on nitrogen-free Fahraeus medium were used. To test the effect of *S. meliloti* inoculation, 4-day-old seedlings were spot-inoculated with a 1 µl drop of *S. meliloti* culture at the zone of emerging root hairs. The inoculation site was marked on the plate. Roots were placed in the incubator for a further 24 h. Roots were excised 20 mm above the tip and the cut end was placed in contact with a small block of agar containing radio-labelled IAA for 6 h. In *Rhizobium* infected roots, the radiolabelled auxin was quantified in a 4 mm segment below the point of inoculation, and

in an equivalent segment, 8–12 mm below the placement of the radio-labelled auxin block, in untreated roots, thus measuring acropetal (i.e. from root base to root tip) auxin transport. All experiments were repeated three times independently with $n > 27$.

ACKNOWLEDGEMENTS

We want to thank Richard Thompsom (INRA-Dijon, France) and Jonathan Clarke (JIC-Norwich, UK) for the identification of *cre1* alleles by TILLING in the frame of the EEC GRAIN LEGUMES project, Marianne Brault-Hernandez for help in some real time RT-PCR experiments, as well as Jason Ng and Britta Winterberg for designing the PIN primers. Nod factors were provided by Fabienne Maillet and Jean Dénarié (LIPM, INRA-CNRS, Castanet-Tolosan). *sickle-1* mutant seeds were provided by Douglas Cook (University of California-Davis, USA). Microscopy was done on the IMAGIF platform (CNRS, Gif sur Yvette, France; Marie Noelle Soler and Suzanne Bolte). Antibodies against *M. truncatula* PINs were developed in the frame of a French ACI program ('cell polarity and organogenesis') involving Béatrice Satiat-Jeuemaitre (CNRS-Gif sur Yvette, France) and Jan Traas (Ecole Normale Supérieure, Lyon, France). We thank the ECOS-Sud program A07B03, the 'Ambassade de France' and the 'Banco Santa Fe Foundation' for providing short-term fellowships to F.A. J.P. was the recipient of a doctoral grant from the 'Ministère de la Recherche et de la Technologie' (France). A.W. was supported by an Australian Postgraduate Award. U.M. was supported by funding from the Australian Research Council through an Australian Research Fellowship (DP0557692) and the Centre of Excellence for Integrative Legume Research (CE0348212). F.F. was supported by a French ANR project, LEGUROOT.

SUPPORTING INFORMATION

Additional Supporting Information may be found in the online version of this article:

Figure S1. Late *cre1* nodulation phenotype.

Figure S2. Expression of the *PRO_{MtRR4}:GUS* transcriptional fusion in *S. meliloti* 1021 inoculated mature nodules.

Figure S3. Expression of *M. truncatula* PIN encoding genes in response to cytokinins.

Figure S4. Differential expression of *M. truncatula* PIN encoding genes between the *cre1-1* mutant and wild-type roots.

Figure S5. Quantification of PIN polar signals obtained in immunolocalization with PIN antibodies.

Table S1. Homology between the peptide used to generate the PIN62 antibody and MtPINs.

Table S2. List of primers and probes used.

Please note: As a service to our authors and readers, this journal provides supporting information supplied by the authors. Such materials are peer-reviewed and may be re-organized for online delivery, but are not copy-edited or typeset. Technical support issues arising from supporting information (other than missing files) should be addressed to the authors.

REFERENCES

Alonso, J.M., Hirayama, T., Roman, G., Nourizadeh, S. and Ecker, J.R. (1999) EIN2, a bifunctional transducer of ethylene and stress responses in Arabidopsis. *Science*, **284**, 2148–2152.

Andriankaja, A., Boisson-Dernier, A., Frances, L., Sauviac, L., Jauneau, A., Barker, D.G. and de Carvalho-Niebel, F. (2007) AP2-ERF transcription factors mediate Nod factor dependent *Mt ENOD11* activation in root hairs via a novel cis-regulatory motif. *Plant Cell*, **19**, 2866–2885.

Ardourel, M., Demont, N., Debelle, F., Maillet, F., de Billy, F., Prome, J.C., Denarie, J. and Truchet, G. (1994) *Rhizobium meliloti* lipooligosaccharide nodulation factors: different structural requirements for bacterial entry into

target root hair cells and induction of plant symbiotic developmental responses. *Plant Cell*, **6**, 1357–1374.

- Benkova, E. and Hejatko, J. (2009) Hormone interactions at the root apical meristem. *Plant Mol. Biol.* **69**, 383–396.
- Blondon, F. (1964) Contribution à l'étude du développement de graminées forragères: Ray-grass et dactyle. *Rev. Gen. Bot.* **71**, 293–381.
- Boisson-Dernier, A., Chabaud, M., Garcia, F., Becard, G., Rosenberg, C. and Barker, D.G. (2001) *Agrobacterium rhizogenes*-transformed roots of *Medicago truncatula* for the study of nitrogen-fixing and endomycorrhizal symbiotic associations. *Mol. Plant Microbe Interact.* **14**, 695–700.
- Boualem, A., Laporte, P., Jovanovic, M., Laffont, C., Plet, J., Combié, J.P., Niebel, A., Crespi, M. and Frugier, F. (2008) MicroRNA166 controls root and nodule development in *Medicago truncatula*. *Plant J.* **54**, 876–887.
- Cary, A.J., Liu, W. and Howell, S.H. (1995) Cytokinin action is coupled to ethylene in its effects on the inhibition of root and hypocotyl elongation in *Arabidopsis thaliana* seedlings. *Plant Physiol.* **107**, 1075–1082.
- Coba de la Pena, T., Frugier, F., McKhann, H.I., Bauer, P., Brown, S., Kondorosi, A. and Crespi, M. (1997) A carbonic anhydrase gene is induced in the nodule primordium and its cell-specific expression is controlled by the presence of *Rhizobium* during development. *Plant J.* **11**, 407–420.
- Crespi, M. and Frugier, F. (2008) *De novo* organ formation from differentiated cells: root nodule organogenesis. *Sci. Signal.* **1**, re11.
- Dello loio, R., Linhares, F.S., Scacchi, E., Casamitjana-Martinez, E., Heidstra, R., Costantino, P. and Sabatini, S. (2007) Cytokinins determine Arabidopsis root-meristem size by controlling cell differentiation. *Curr. Biol.* **17**, 678–682.
- Dello loio, R., Nakamura, K., Moubayidin, L., Perilli, S., Taniguchi, M., Morita, M.T., Aoyama, T., Costantino, P. and Sabatini, S. (2008) A genetic framework for the control of cell division and differentiation in the root meristem. *Science*, **322**, 1380–1384.
- Friml, J., Benková, E., Mayer, U., Palme, K. and Muster, G. (2003) Automated whole mount localisation techniques for plant seedlings. *Plant J.* **34**, 115–124.
- Frugier, F., Kosuta, S., Murray, J.D., Crespi, M. and Szczygłowski, K. (2008) Cytokinin: secret agent of symbiosis. *Trends Plant Sci.* **13**, 115–120.
- Gleason, C., Chaudhuri, S., Yang, T.B., Munoz, A., Poovaiah, B.W. and Oldroyd, G.E.D. (2006) Nodulation independent of rhizobia induced by a calcium-activated kinase lacking autoinhibition. *Nature*, **441**, 1149–1152.
- Gonzalez-Rizzo, S., Crespi, M. and Frugier, F. (2006) The *Medicago truncatula* CRE1 cytokinin receptor regulates lateral root development and early symbiotic interaction with *Sinorhizobium meliloti*. *Plant Cell*, **18**, 2680–2693.
- Gresshoff, P.M., Lohar, D., Chan, P.K., Biswas, B., Jiang, Q., Reid, D., Ferguson, B. and Stacey, G. (2009) Genetic analysis of ethylene regulation of legume nodulation. *Plant Sign. Behav.* **4**, 818–823.
- Heckmann, A.B., Lombardo, F., Miwa, H., Perry, J.A., Bunnewell, S., Parniske, M., Wang, T.L. and Downie, J.A. (2006) *Lotus japonicus* nodulation requires two GRAS domain regulators, one of which is functionally conserved in a non-legume. *Plant Physiol.* **142**, 1739–1750.
- Heidstra, R., Yang, W.C., Yalcin, Y., Peck, S., Emons, A.M., van Kammen, A. and Bisseling, T. (1997) Ethylene provides positional information on cortical cell division but is not involved in Nod factor-induced root hair tip growth in *Rhizobium-legume* interaction. *Development*, **124**, 1781–1787.
- Huo, X., Schnabel, E., Hughes, K. and Frugoli, J. (2006) RNAi phenotypes and the localization of a protein::GUS fusion imply a role for *Medicago truncatula* PIN genes in nodulation. *J. Plant Growth Regul.* **25**, 156–165.
- Hwang, D., Chen, H.C. and Sheen, J. (2002) Two-component signal transduction pathways in Arabidopsis. *Plant Physiol.* **129**, 500–515.
- Kalo, P., Gleason, C., Edwards, A. et al. (2005) Nodulation signaling in legumes requires NSP2, a member of the GRAS family of transcriptional regulators. *Science*, **308**, 1786–1789.
- Laplaze, L., Benkova, E. and Casimiro, I. (2007) Cytokinins act directly on lateral root founder cells to inhibit root initiation. *Plant Cell*, **19**, 3889–3900.
- Le Signor, C., Savoie, V., Aubert, G. et al. (2009) Optimizing TILLING populations for reverse genetics in *Medicago truncatula*. *Plant Biotechnol. J.* **7**, 430–441.
- Libault, M., Farmer, A. and Brechenmacher, L., et al. (2010) Complete transcriptome of the soybean root hair cell, a single cell model, and its alteration in response to *Bradyrhizobium japonicum* infection. *Plant Physiol.* **152**, 541–552.

- Libault, M., Joshi, T., Takahashi, K., Hurley-Sommer, A., Puricelli, K., Blake, S., Xu, D., Nguyen, H.T. and Stacey, G. (2009) Large-scale analysis of putative soybean regulatory gene expression identifies a Myb gene involved in soybean nodule development. *Plant Physiol.* **151**, 1207–1220.
- Lohar, D.P., Schaff, J.E., Laskey, J.G., Kieber, J.J., Bilyeu, K.D. and Bird, D.M. (2004) Cytokinins play opposite roles in lateral root formation, and nematode and rhizobial symbioses. *Plant J.* **38**, 203–214.
- Lohar, D.P., Sharopova, N., Endre, G., Penuela, S., Samac, D., Town, C., Silverstein, K.A. and Vanden Bosch, K.A. (2006) Transcript analysis of early nodulation events in *Medicago truncatula*. *Plant Physiol.* **140**, 221–234.
- Madsen, L.H., Tirichine, L., Jurkiewicz, A., Sullivan, J.T., Heckmann, A.B., Bek, A.S., Ronson, C.W., James, E.K. and Stougaard, J. (2010) The molecular network governing nodule organogenesis and infection in the model legume *Lotus japonicus*. *Nat. Commun.* **1**, 1–12.
- Magori, S., Oka-Kira, E., Shibata, S., Umehara, Y., Kouchi, H., Hase, Y., Tanaka, A., Sato, S., Tabata, S. and Kawaguchi, M. (2009) Too much love, a root regulator associated with the long-distance control of nodulation in *Lotus japonicus*. *Mol. Plant-Microbe Interact.* **22**, 259–268.
- Marsh, J.F., Rakocevic, A., Mitra, R.M., Brocard, L., Sun, J., Eschstruth, A., Long, S.R., Schultze, M., Ratet, P. and Oldroyd, G.E. (2007) *Medicago truncatula* NIN is essential for rhizobial-independent nodule organogenesis induced by autoactive calcium/calmodulin-dependent protein kinase. *Plant Physiol.* **144**, 324–335.
- Mathesius, U., Schlaman, H.R., Spaink, H.P., Of Sautter, C., Rolfe, B.G. and Djordjevic, M.A. (1998) Auxin transport inhibition precedes root nodule formation in white clover roots and is regulated by flavonoids and derivatives of chitin oligosaccharides. *Plant J.* **14**, 23–34.
- Middleton, P.H., Jakab, J., Penmetsa, R.V. *et al.* (2007) An ERF transcription factor in *Medicago truncatula* that is essential for Nod factor signal transduction. *Plant Cell*, **19**, 1221–1234.
- Muller, B. and Sheen, J. (2008) Cytokinin and auxin interaction in root stem-cell specification during early embryogenesis. *Nature*, **453**, 1094–1097.
- Murakami, Y., Miwa, H., Imaizumi-Anraku, H., Kouchi, H., Downie, J.A., Kawaguchi, M. and Kawasaki, S. (2006) Positional cloning identifies *Lotus japonicus* NSP2, a putative transcription factor of the GRAS family, required for *NIN* and *ENOD40* gene expression in nodule initiation. *DNA Res.* **13**, 255–265.
- Murray, J.D., Karas, B.J., Sato, S., Tabata, S., Amyot, L. and Szczyglowski, K. (2007) A cytokinin perception mutant colonized by *Rhizobium* in the absence of nodule organogenesis. *Science*, **315**, 101–104.
- Negi, S., Ivanchenko, M.G. and Muday, G.K. (2008) Ethylene regulates lateral root formation and auxin transport in *Arabidopsis thaliana*. *Plant J.* **55**, 175–187.
- Oldroyd, G.E. and Downie, J.A. (2008) Coordinating nodule morphogenesis with rhizobial infection in legumes. *Annu. Rev. Plant Biol.* **59**, 519–546.
- Penmetsa, R.V. and Cook, D.R. (1997) A legume ethylene-insensitive mutant hyperinfected by its rhizobial symbiont. *Science*, **275**, 527–530.
- Penmetsa, R.V., Frugoli, J.A., Smith, L.S., Long, S.R. and Cook, D.R. (2003) Dual genetic pathways controlling nodule number in *Medicago truncatula*. *Plant Physiol.* **131**, 998–1008.
- Penmetsa, R.V., Uribe, P., Anderson, J. *et al.* (2008) The *Medicago truncatula* ortholog of *Arabidopsis EIN2*, *sickle*, is a negative regulator of symbiotic and pathogenic microbial associations. *Plant J.* **55**, 580–595.
- Petrasek, J. and Friml, J. (2009) Auxin transport routes in plant development. *Development*, **136**, 2675–2688.
- Pichon, M., Journet, E.P., Dedieu, A., de Billy, F., Truchet, G. and Barker, D.G. (1992) *Rhizobium meliloti* elicits transient expression of the early nodulin gene *ENOD12* in the differentiating root epidermis of transgenic alfalfa. *Plant Cell*, **4**, 1199–1211.
- Quandt, H.J., Puhler, A. and Broer, I. (1993) Transgenic root nodules of *Vicia hirsuta*: a fast and efficient system for the study of gene expression in indeterminate-type nodules. *Mol. Plant Microbe Interact.* **6**, 699–706.
- Roche, P., Debelle, F., Maillet, F., Lerouge, P., Faucher, C., Truchet, G., Dénarié, J. and Promé, J.C. (1991) Molecular basis of symbiotic host specificity in *Rhizobium meliloti*: *nodH* and *nodPQ* genes encode the sulfation of lipo-oligosaccharide signals. *Cell*, **67**, 1131–1143.
- Ruzicka, K., Simaskova, M., Duclercq, J., Petrasek, J., Zazimalova, E., Simon, S., Friml, J., Van Montagu, M.C. and Benkova, E. (2009) Cytokinin regulates root meristem activity via modulation of the polar auxin transport. *Proc. Natl Acad. Sci. USA*, **106**, 4284–4289.
- Schauser, L., Handberg, K., Sandal, N., Stiller, J., Thykjaer, T., Pajuelo, E., Nielsen, A. and Stougaard, J. (1998) Symbiotic mutants deficient in nodule establishment identified after T-DNA transformation of *Lotus japonicus*. *Mol. Genet. Genomics*, **259**, 414–423.
- Schnabel, E.L. and Frugoli, J. (2004) The PIN and LAX families of auxin transport genes in *Medicago truncatula*. *Mol. Genet. Genomics*, **272**, 420–432.
- Smit, P., Raedts, J., Portyanko, V., Debelle, F., Gough, C., Bisseling, T. and Geurts, R. (2005) NSP1 of the GRAS protein family is essential for rhizobial Nod factor-induced transcription. *Science*, **308**, 1789–1791.
- Tirichine, L., Sandal, N., Madsen, L.H., Radutoiu, S., Albrektsen, A.S., Sato, S., Asamizu, E., Tabata, S. and Stougaard, J. (2007) A gain-of-function mutation in a cytokinin receptor triggers spontaneous root nodule organogenesis. *Science*, **315**, 104–107.
- Titapiwatanakun, B. and Murphy, A.S. (2009) Post-transcriptional regulation of auxin transport proteins: cellular trafficking, protein phosphorylation, protein maturation, ubiquitination, and membrane composition. *J. Exp. Bot.* **60**, 1093–1107.
- Truchet, G., Debelle, F., Vasse, J., Terzaghi, B., Garnerone, A.M., Rosenberg, C., Batut, J., Maillet, F. and Denarie, J. (1985) Identification of a *Rhizobium meliloti* pSym2011 region controlling the host specificity of root hair curling and nodulation. *J. Bacteriol.* **164**, 1200–1210.
- Valoczi, A., Varallyay, E., Kauppinen, S., Burgyan, J. and Havelda, Z. (2006) Spatio-temporal accumulation of microRNAs is highly coordinated in developing plant tissues. *Plant J.* **47**, 140–151.
- Vandesompele, J., De Preter, K., Pattyn, F., Poppe, B., Van Roy, N., De Paepe, A. and Speleman, F. (2002) Accurate normalization of real-time quantitative RT-PCR data by geometric averaging of multiple internal control genes. *Genome Biol.* **3**, research0034.1-0034.11.
- Vasse, J., de Billy, F., Camut, S. and Truchet, G. (1990) Correlation between ultrastructural differentiation of bacteroids and nitrogen fixation in alfalfa nodules. *J. Bacteriol.* **172**, 4295–4306.
- Vernie, T., Moreau, S., de Billy, F., Plet, J., Combier, J.P., Rogers, C., Oldroyd, G., Frugier, F., Niebel, A. and Gamas, P. (2008) EFD is an ERF transcription factor involved in the control of nodule number and differentiation in *Medicago truncatula*. *Plant Cell*, **20**, 2696–2713.
- Wasson, A.P., Pellerone, F.I. and Mathesius, U. (2006) Silencing the flavonoid pathway in *Medicago truncatula* inhibits root nodule formation and prevents auxin transport regulation by rhizobia. *Plant Cell*, **18**, 1617–1629.
- Werner, T. and Schumling, T. (2009) Cytokinin action in plant development. *Curr. Opin. Plant Biol.* **12**, 527–538.